Lattice vibrations of a single-wall boron nitride nanotube

Gun Sang Jeon
Department of Physics and Astronomy, Seoul National University, Seoul 151-747, Korea

G. D. Mahan
Department of Physics, Pennsylvania State University, University Park, Pennsylvania 16802, USA
(Received 17 October 2008; revised manuscript received 20 January 2009; published 24 February 2009)

We construct a simple model which describes the lattice dynamics of a single-wall boron nitride nanotube. The model includes short-range interactions between nearest and second-nearest neighbors as well as long-range Coulomb interactions between polar atoms. It is clearly shown that flexure modes exist in boron nitride nanotubes consisting of polar atoms. We also find that the frequency of the radial breathing mode is inversely proportional to the tube radius R and that the lowest optical mode displays the radius dependence of $1/R^2$ consistent with earlier calculations.

DOI: 10.1103/PhysRevB.79.085424 PACS number(s): 63.22.−m, 78.30.Na

I. INTRODUCTION

The discovery of a carbon nanotube (CNT) (Ref. 1) initiated extensive studies on the nanotube structures for a variety of applications in nanotechnology.[2–5] Although CNT has been the most popular nanotube structure in the studies, there have been many other structural analogs of a CNT. One important analog is a boron nitride nanotube (BNNT).

Shortly after a BNNT was predicted to exist by the tight-binding calculation[6] and the *ab initio* calculation,[7] BNNTs were first synthesized[8] and have been produced by several methods in the forms of both single-wall and multiwall nanotubes.[5] The striking difference between BNNTs and CNTs is that BNNTs are always semiconducting[9] with wide band gap ≈ 5.5 eV, while CNTs are semiconducting or metallic depending on their chirality. Further, the fact that boron nitride layers are more stable than graphatic carbon structure leads to the expectation of better structural properties of BNNTs. Such peculiar properties of BNNTs motivated recent studies on various possible applications such as gas adsorption nanostructures[10] and electrical nanocables.[11]

The Raman and the infrared spectroscopies have proved to provide an effective way for the characterization of nanotube samples, which requires accurate predictions of lattice vibrational modes in nanotubes. For CNTs, there have been a number of theoretical studies on the phonon spectra.[12–30] Particularly, the radial breathing mode is useful in identifying carbon nanotubes experimentally since the mode is strongly dependent on the tube diameter.[27–30]

The existence of flexure modes has been another interesting issue in the lattice dynamics of CNTs. The approaches based on elastic theory[31,32] predicted that four low-frequency modes exist in CNTs; two of them are longitudinal-acoustic and torsional modes, which are proportional to the wave number q along the tube axis, while the other two are flexure modes which exhibit quadratic dependence on q. On the other hand, many calculations[12–16] concluded that all four low-frequency modes are acoustical. Some refined calculations[23–26] recovered flexure modes, which was confirmed in recent molecular-dynamic calculations of heat conduction in CNTs.[33]

The lattice vibrations in BNNTs have also been studied in several ways such as a tight-binding model,[34] a valence-shell model,[35] and an *ab initio* calculation.[36] All the calculations produced the same general properties: the high-frequency modes around 1370 cm^{-1} which are consistent with Raman observations,[37,38] the radial breathing modes which are inversely proportional to the tube radius, and four low-frequency modes. The last two properties are similar to those of CNTs. An interesting thing is that none of them observed clearly flexure modes, which are believed to be the general properties of a cylindrical geometry.[31,32]

The main purpose of this work is to devise a simple model which can describe well the lattice dynamics of BNNTs. The essential ingredient of the model is the inclusion of Coulomb interactions between the atoms since BNNTs are polar materials. In our model, we incorporate short-range interactions between the first- and the second-nearest neighbors as well as long-range Coulomb interactions. Within the model, we construct the dynamical equation for the displacements of atoms, calculating the phonon spectrum of BNNTs. It describes correctly low-frequency phonons; the quadratic dependence of flexure modes on the wave number is demonstrated. The frequency of the radial breathing mode is shown to be v_L/R, where v_L is the velocity of the longitudinal-acoustical phonon and R is the tube radius; this was predicted by the elastic theory.[31] It is also found that the lowest optical phonon exhibits $1/R^2$ dependence.

This paper is organized as follows. We describe our model and present the results for armchair BNNTs in Sec. II. Section III is devoted to the results of zigzag BNNTs. A brief summary is given in Sec. IV and the zero-stress condition which is crucial in the inclusion of Coulomb interactions is detailed in the Appendix.

II. ARMCHAIR BORON NITRIDE NANOTUBE

A BNNT is composed of two kinds of atoms: boron (B) and nitrogen (N). The main difference of the equilibrium geometry of BNNT from that of CNT is a buckling of the boron-nitrogen bond. From the *ab initio* structural studies,[7,36,39–41] it has been shown that all the B atoms are arranged in one cylinder while all the N atoms lie in a con-

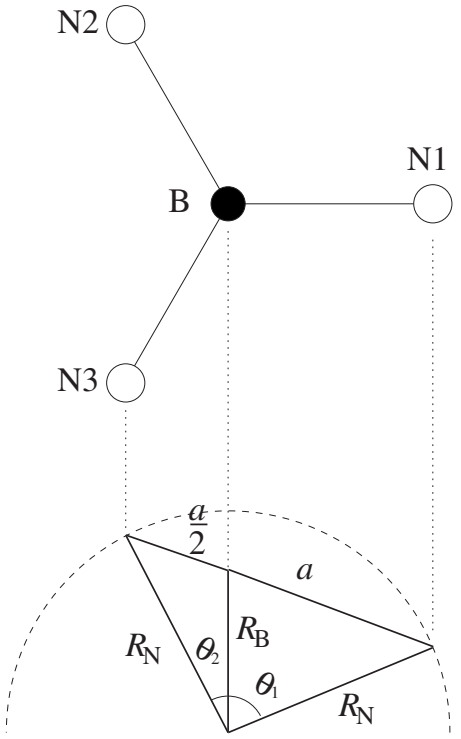

FIG. 1. Three neighbors of boron atom at site B in armchair boron nitride nanotubes.

centric one of larger radius. Each B atom tends to keep the planar sp^2 bonding geometry.[7,36] The buckling distance (the distance between the inner and the outer cylinders) is smaller than 0.1 Å for the tube of radius ~2.5 Å and decreases monotonically with the tube radius. In some phonon calculation,[35] such small buckling distance was neglected.

For an armchair BNNT, we take a primitive unit cell, which has one B atom and one N atom, respectively, at

$$\boldsymbol{R}_{\mathrm{B}} = \{R_{\mathrm{B}}, 0, 0\}, \tag{1}$$

$$\boldsymbol{R}_{\mathrm{N1}} = \{R_{\mathrm{N}}, \theta_1, 0\} \tag{2}$$

in cylindrical coordinates $\{\rho, \theta, z\}$. The B atom has three nearest neighbors as drawn in Fig. 1. The positions of the other two N atoms are

$$\boldsymbol{R}_{\mathrm{N2}} = \{R_{\mathrm{N}}, -\theta_2, c_A\}, \tag{3}$$

$$\boldsymbol{R}_{\mathrm{N3}} = \{R_{\mathrm{N}}, -\theta_2, -c_A\}. \tag{4}$$

A B atom is assumed to be placed at the center of the equilateral triangle, which is formed by its three neighboring N atoms (N1, N2, and N3 in Fig. 1). The bond length of B-N is given by $a=1.44$ Å.[36,39,40] In achiral nanotubes, we have B-N bonds of two types: B-N1 and B-N2 (or B-N3) in Fig. 1. The bond lengths of two types are slightly different. However, the difference is ~0.03 Å even for the smallest stable nanotubes,[39,40] which we neglect in this work.

In this approximation, we obtain the expression for two radii (R_{N} and R_{B}) for an (N,N) armchair BNNT,

$$R_{\mathrm{N}} = \frac{3a}{4\sin(\tilde{\theta}/2)},$$

$$R_{\mathrm{B}} = a\sqrt{\frac{9}{16\sin^2(\tilde{\theta}/2)} - \frac{1}{2}}, \tag{5}$$

along with $\theta_1 + \theta_2 = \frac{\pi}{N} \equiv \tilde{\theta}$ and $c_A = \frac{\sqrt{3}}{2}a$. It is noted that the buckling distance $R_{\mathrm{N}} - R_{\mathrm{B}}$ is inversely proportional to the tube radius $R \equiv (R_{\mathrm{N}} + R_{\mathrm{B}})/2$,

$$R_{\mathrm{N}} - R_{\mathrm{B}} = \frac{1}{R_{\mathrm{N}} + R_{\mathrm{B}}}\frac{a^2}{2} \propto \frac{a^2}{R}, \tag{6}$$

which is consistent with an earlier *ab initio* calculation.[36] For $N \gg 1$, the buckling distance is given by

$$R_{\mathrm{N}} - R_{\mathrm{B}} = \frac{\pi}{6N}a + \mathcal{O}\left(\frac{1}{N^2}\right). \tag{7}$$

The values of the outer radius R_{N} used in our model are almost the same as earlier *ab initio* results,[39,40] while the inner radius R_{B} is slightly underestimated with less than 2% errors for $N \geq 6$.

A big unit cell which is a basic block in the z direction contains $4N$ atoms and can be constructed from a primitive cell by two transformations,

$$T_1[\{\rho, \theta, z\}] = \{\rho, \theta + \tilde{\theta}, z - c_A\}, \tag{8}$$

$$T_2[\{\rho, \theta, z\}] = \{\rho, \theta + \tilde{\theta}, z + c_A\}. \tag{9}$$

The transformations $(T_1 + T_2)^{n_1} T_2^{n_2}$ with $n_1 = 0, \ldots, N-1$ and $n_2 = 0, 1$ map a primitive cell to a big unit cell. The entire nanotube is obtained by the periodic placement of big unit cells with period $2c_A$.

To describe phonons of a BNNT, we consider the displacements $\boldsymbol{Q}_{\mathrm{B}}$ and $\boldsymbol{Q}_{\mathrm{N}}$ of atoms in three dimensions. Phonon states are classified by two wave numbers: q in the z direction and α in the azimuthal direction.[23,24] For an infinitely long tube, q is a continuous variable in the range $[-\pi/2c_A, \pi/2c_A]$. The azimuthal wave number α takes an integer satisfying $|\alpha| \leq N/2$. For an even N, $\alpha = \pm N/2$ are equivalent to each other.

We include both short-range interactions and long-range Coulomb interactions between polar atoms. Bond-stretching interactions between nearest-neighbor atoms and between second-nearest-neighbor atoms are taken into account as short-range interactions. The two kinds of bond-stretching interactions are parametrized by its first and second derivatives (ϕ_1', ϕ_1'') and (ϕ_2', ϕ_2''), respectively. The other crucial interactions are electrostatic interactions between polar atoms since a BNNT is a polar material. We include Coulomb interactions with dielectric constant ϵ among all B atoms with charge $+Ze$ and N atoms with charge $-Ze$. The full-range Coulomb interactions are incorporated in the same way as used in Ref. 24. The first derivatives of bond-stretching interactions are restricted by a zero-stress condition for the equilibrium lattice parameter a.[24,42,43] In our model, we set $\phi_2' = 0$ for simplicity and ϕ_1' is determined by

TABLE I. Parameters employed in our model for boron nitride nanotubes. The first derivatives of bond-stretching interactions ϕ_1' and ϕ_2' are given by a zero-stress condition. For simplicity, we set $\phi_2'=0$.

ϕ_1'' (10^4 dyn cm^{-1})	ϕ_2'' (10^4 dyn cm^{-1})	Z^2/ϵ
63	5.0	1.1

the strength of Coulomb interactions. The derivation of the relations is detailed in the Appendix. In Table I we summarize the values of the parameters used in our model, which are obtained by fitting to *ab initio* and experimental data on zone-center optical phonons[36–38] in the limit of large tube radius.

For each pair of (q,α), we construct the total dynamical equation in the form,

$$\omega^2\begin{pmatrix} m_B & 0 \\ 0 & m_N \end{pmatrix}\begin{pmatrix} \boldsymbol{Q}_B \\ \boldsymbol{Q}_N \end{pmatrix} = \hat{\boldsymbol{D}}(q,\alpha)\begin{pmatrix} \boldsymbol{Q}_B \\ \boldsymbol{Q}_N \end{pmatrix}, \tag{10}$$

where $\boldsymbol{Q}_B$ and $\boldsymbol{Q}_N$ are the displacements of B and N atoms in a primitive cell and all the interactions are contained in a dynamical matrix $\hat{\boldsymbol{D}}(q,\alpha)$. The above equations can be written as

$$\omega^2\begin{pmatrix} \boldsymbol{Q}_B' \\ \boldsymbol{Q}_N' \end{pmatrix} = \boldsymbol{M}_{-1/2}\boldsymbol{D}(q,\alpha)\boldsymbol{M}_{-1/2}\begin{pmatrix} \boldsymbol{Q}_B' \\ \boldsymbol{Q}_N' \end{pmatrix}, \tag{11}$$

with

$$\boldsymbol{M}_{-1/2} \equiv \begin{pmatrix} m_B^{-1/2} & 0 \\ 0 & m_N^{-1/2} \end{pmatrix} \tag{12}$$

and

$$\begin{pmatrix} \boldsymbol{Q}_B' \\ \boldsymbol{Q}_N' \end{pmatrix} \equiv \begin{pmatrix} m_B^{1/2}\boldsymbol{Q}_B \\ m_N^{1/2}\boldsymbol{Q}_N \end{pmatrix}. \tag{13}$$

We solve the secular equation,

$$\det[\omega^2 1 - \boldsymbol{M}_{-1/2}\boldsymbol{D}(q,\alpha)\boldsymbol{M}_{-1/2}] = 0 \tag{14}$$

to obtain the phonon frequencies $\omega_n(q,\alpha)$ of a BNNT with a band index $n=1,2,\ldots,6$.

The full phonon dispersion is displayed in Fig. 2(a) for a (10,10) armchair BNNT. Four optical phonons of $\alpha=0$ are at the frequencies 180, 840, 1368, and 1375 cm^{-1}. The first phonon of frequency 180 cm^{-1} is a radial breathing mode. The second phonon of frequency 840 cm^{-1} is a tube version of the out-of-plane optical phonon in a BN flat sheet, whereas the other two modes correspond to longitudinal and transverse in-plane optical phonons of a BN flat sheet, respectively. The low-frequency mode of $\alpha=2$ is at 6.1 cm^{-1}.

The larger-scale presentation of low-frequency behavior in Fig. 2(b) demonstrates four gapless mode at $q=0$: two degenerate transverse modes for $\alpha=\pm1$, longitudinal, and torsional phonons. The latter two phonons are acoustic exhibiting linear dependence on the wave number q for small

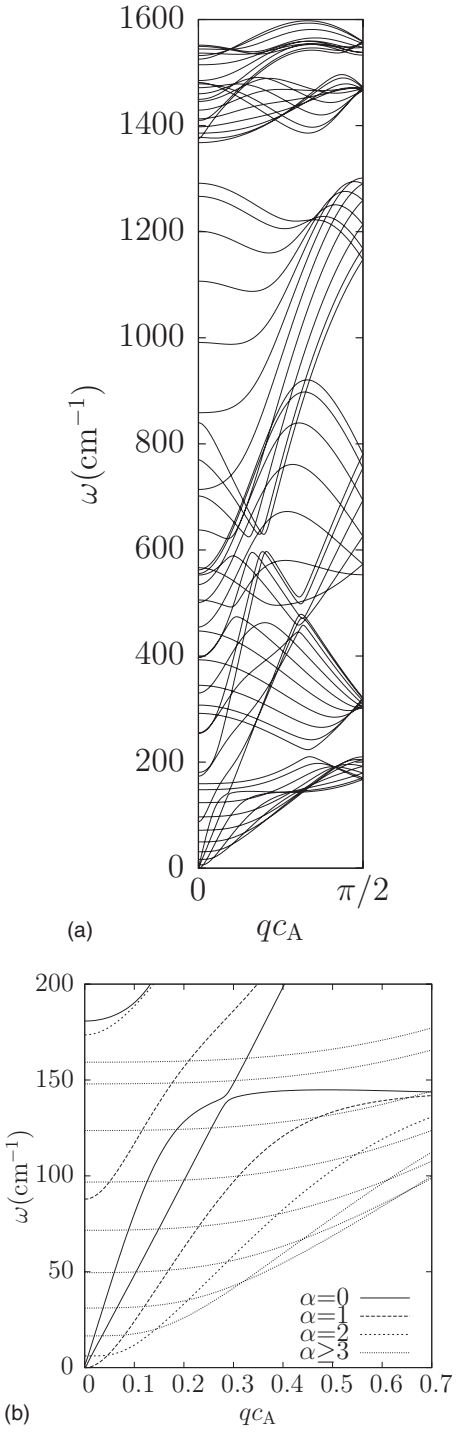

FIG. 2. (a) Phonons in a (10,10) armchair BNNT. (b) Larger-scale presentation of the region at low frequency and small wave vector.

wave numbers. The velocities of the two acoustic phonons are $v_L \approx 20$ km/s and $v_T \approx 11$ km/s, which is in good agreement with earlier works.[34]

The behavior of the transverse modes with $\alpha=\pm1$ is interesting. In earlier studies,[34–36] it was unclear whether the transverse modes exhibit linear or quadratic dependence on the wave number. The valence-shell model[35] showed a linear dependence on the wave number. Tight-binding calculation[34]

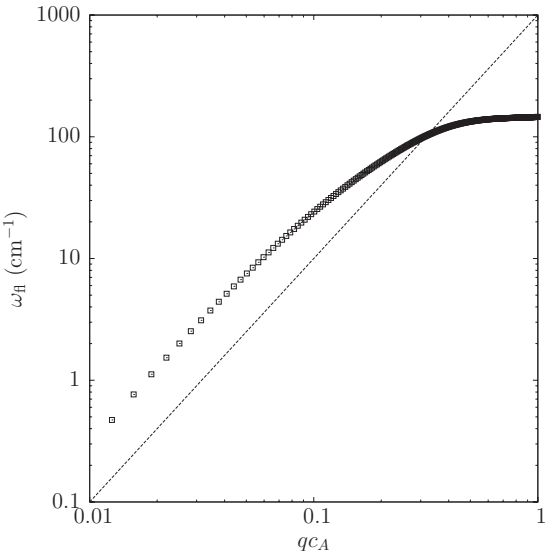

FIG. 3. The log-log plot of the frequency of a flexure mode with $\alpha=1$ versus the wave number q. It clearly exhibits a quadratic dependence of the frequency on the wave number q for small q. The dashed line is a guide for q^2 dependence.

could not clarify the issue due to the numerical accuracy, which was not clearly resolved in the *ab initio* calculation.[36] The log-log plot in Fig. 3 demonstrates the clear quadratic dependence of the mode on q at small wave numbers; this indicates the existence of flexure modes in an armchair BNNT consistent with the elastic theory.[31,32]

We also compute the dependence of the frequency of a radial breathing mode as a function of the tube radius R. As is shown in Fig. 4, it is inversely proportional to R consistent with earlier results.[34–36] The best fit is $A(R/R_0)^{-\delta}$ with $R_0 \equiv 1$ Å, $A=1230\pm2$ cm^{-1}, and $\delta=0.9956\pm0.0004$. The

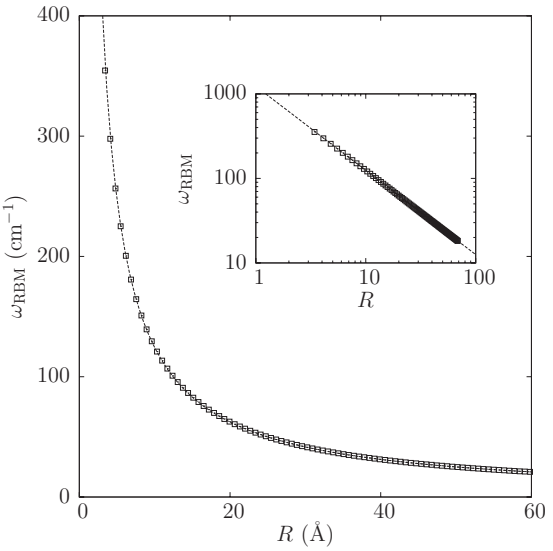

FIG. 4. The frequency of a radial breathing mode as a function of radius for armchair BNNT. The dashed line is a fitting curve $f(R)=A(R/R_0)^{-\delta}$ with $R_0\equiv1$ Å, $A=1230\pm2$ cm^{-1}, and $\delta=0.995\,6\pm0.000\,4$. The inset shows the log-log plot of the frequency of a radial breathing mode.

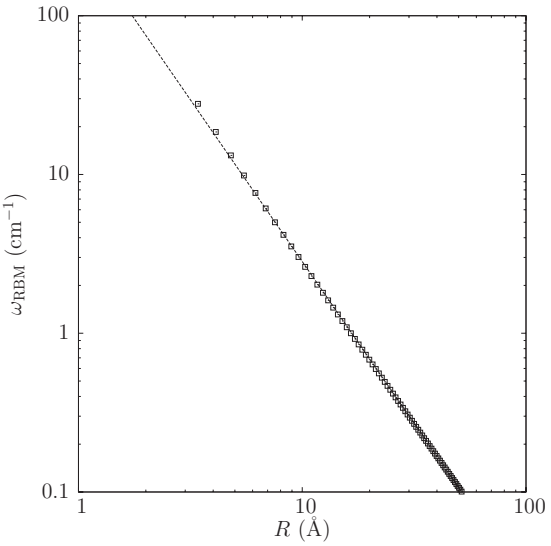

FIG. 5. The frequency of the low-frequency mode with $\alpha=2$ as a function of radius for armchair BNNT. The dashed line is a fitting curve $f(R)=A(R/R_0)^{-\delta}$ with $R_0\equiv1$ Å, $A=309\pm3$ cm^{-1}, and $\delta=2.04\pm0.01$.

proportional constant A is comparable to—but slightly larger than—earlier theoretical estimations for BNNT, 850–1100 from various approaches such as the tight-binding model,[34] the valence shell model,[35] and the *ab initio* calculations.[36,41] Indeed the phonon frequencies of the radial breathing modes are in good agreement with the behavior v_L/R, which was shown in the elastic theory.[31] The dependence of the low-frequency mode with $\alpha=2$ on the tube radius R is also interesting. Unlike the radial breathing mode, it exhibits a decrease roughly proportional to $1/R^2$ as shown in Fig. 5; this reproduces the *ab initio* results.[19,36]

III. ZIGZAG CARBON NANOTUBE

In this section, we study $(N,0)$ zigzag nanotubes within the same model. In a primitive unit cell of an $(N,0)$ zigzag BNNT, we have two atoms at

$$\boldsymbol{R}_{\mathrm{B}} = \{R_{\mathrm{B}},0,0\}, \tag{15}$$

$$\boldsymbol{R}_{\mathrm{N1}} = \left\{R_{\mathrm{N}},0,\frac{2}{3}c_Z\right\}. \tag{16}$$

The positions of the other two N atoms nearest to the B atom are

$$\boldsymbol{R}_{\mathrm{N2}} = \left\{R_{\mathrm{N}},-\frac{\theta_Z}{2},-\frac{1}{3}c_Z\right\}, \tag{17}$$

$$\boldsymbol{R}_{\mathrm{N3}} = \left\{R_{\mathrm{N}},\frac{\theta_Z}{2},-\frac{1}{3}c_Z\right\}. \tag{18}$$

From the assumption that B atom is placed at the center of three N atoms (N1, N2, and N3), one can obtain for an $(N,0)$ zigzag BNNT

$$\theta_Z = \frac{2\pi}{N}, \tag{19}$$

$$R_N = \frac{\sqrt{3}a}{2\sin(\theta_Z/2)}, \tag{20}$$

$$R_B = \frac{1}{3}R_N\left(1 + 2\cos\frac{\theta_Z}{2}\right), \tag{21}$$

$$c_Z = \frac{3}{2}a\sqrt{1 - \frac{[1-\cos(\theta_Z/2)]^2}{3\sin^2(\theta_Z/2)}}. \tag{22}$$

The deviation of c_Z from $3a/2$ due to the buckling is less than 1% for $N>5$.

It is also convenient to construct a big unit cell from a primitive cell for a zigzag BNNT. Applying the transformations $T_1^{n_1}T_2^{n_2}$ with $n_1=0,1$, $n_2=0,\ldots,N-1$, and

$$T_1[\{\rho,\theta,z\}] = \{\rho,\theta+\theta_z,z\}, \tag{23}$$

$$T_2[\{\rho,\theta,z\}] = \{\rho,\theta+\theta_z/2,z+c_Z\}, \tag{24}$$

we can map a primitive cell onto a big unit cell composed of $4N$ atoms.

We employ the same parameters as in armchair nanotubes and compute the phonon dispersion for a (17,0) zigzag BNNT. The full and low-frequency phonon spectrum is shown in Figs. 6(a) and 6(b). The optical phonons of $\alpha=0$ are at the frequencies 184, 840, 1368, and 1375 cm^{-1}. At low frequencies, we also find two acoustic modes and two (degenerate) flexure modes at small wave vector q. The velocities of the two acoustic phonons are $v_T \approx 11$ km/s and $v_L \approx 20$ km/s, and flexure modes exhibit a quadratic dependence on q. The low-frequency mode of $\alpha=2$ is at 6.3 cm^{-1}. The frequency ω_{RBM} of the radial breathing mode for $(N,0)$ zigzag nanotubes displays the same behavior $\sim 1/R$ as in armchair tubes. The best fit to the function $f(R) = A(R/R_0)^{-\delta}$ ($R_0 \equiv 1$ Å) is obtained with $A=1231\pm2$ cm^{-1} and $\delta=0.995\,9\pm0.000\,3$. In fact, both curves of radial breathing mode frequency versus a tube radius for armchair and zigzag BNNTs are almost overlapped as reported earlier.[34,35]

IV. SUMMARY

We have studied the lattice dynamics of a single-wall boron nitride nanotube, paying particular attention to the low-frequency modes. We have devised a simple model which incorporated short-range interactions between first- and second-nearest-neighbor atoms as well as long-range Coulomb interactions between polar atoms. Our model has proved to describe correctly the behavior of flexure modes which are transverse gapless modes of the nanotube and display quadratic dependence on the wave number for small wave numbers. We also reproduced the radius dependence of the radial breathing mode and the lowest optical phonon with $\alpha=2$.

ACKNOWLEDGMENTS

This work was supported in part by the Asia Pacific Center for Theoretical Physics. G.S.J. acknowledges the support from the Korea Research Foundation Grant funded by the Korean Government (MOEHRD, Basic Research Promotion Fund) (Grant No. KRF-2007-314-C00075).

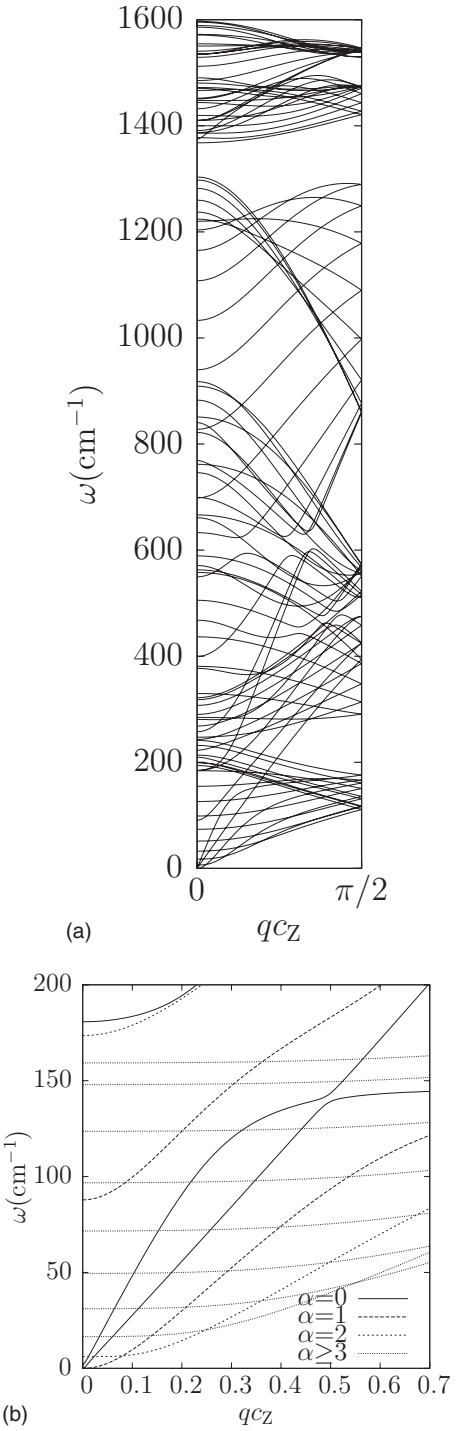

FIG. 6. (a) Phonons in a (17,0) zigzag BNNT. (b) Larger-scale presentation of the region at low frequency and small wave vector.

APPENDIX

In this appendix, we derive the expression for $\phi_1'(a)$ from the zero-stress condition. The total energy of an entire tube is given by

$$E(a) = \frac{1}{2}\sum_{\alpha\neq\beta}\left[\phi_1(\boldsymbol{r}_\alpha - \boldsymbol{r}_\beta) + \frac{e^2 Z_\alpha Z_\beta}{\epsilon|\boldsymbol{r}_\alpha - \boldsymbol{r}_\beta|}\right], \tag{A1}$$

where α and β are the indices of atoms in an entire nanotube and $\boldsymbol{r}_\alpha$ and Z_α denote the equilibrium position and the charge of atom α, respectively. ϕ_1 is a bond-stretching force between the first-nearest-neighbor atoms. For simplicity, we neglect the change in all other energies due to the variation of a. The expression for the total energy can be simplified as

$$E(a) = \frac{1}{2}N_z\left[12N\phi_1(a) + \frac{e^2}{\epsilon}\sum_{i,j} Z_i Z_j \bar{V}_{ij}(a)\right], \tag{A2}$$

where

$$\bar{V}_{ij}(a) \equiv \sum_{n=-\infty}^{\infty} \frac{e^{iq2nc}}{\sqrt{\rho_{ij}^2 + (z_{ij} - 2nc)^2}}\Bigg|_{q\to 0} \tag{A3}$$

with $\rho_{ij}^2 = \rho_i^2 + \rho_j^2 - 2\rho_i\rho_j\cos(\theta_i - \theta_j)$ and $z_{ij} \equiv z_i - z_j$. N_z is the number of big unit cells in a BNNT and the summation of i and j runs over the atoms in a big unit cell of $4N$ atoms for (N,N) armchair or $(N,0)$ zigzag BNNT.

From the zero-stress condition $dE(a)/da = 0$ for equilibrium geometry, one can obtain

$$\phi_1'(a) = -\frac{e^2}{12N}\sum_{i,j} Z_i Z_j \frac{d\bar{V}_{ij}}{da} = -\frac{e^2}{6}\sum_b Z_b \sum_j Z_j \frac{d\bar{V}_{ij}}{da}, \tag{A4}$$

where the summation b runs over the atoms in a primitive cell. (Note that $\Sigma_i = 2N\Sigma_b$.) It is straightforward to calculate the derivative of pair Coulomb interaction with respect to a. For $i=j$,

$$\frac{d\bar{V}_{ij}}{da} = \frac{1}{ac}[\ln(2qc) - 1]. \tag{A5}$$

For $\rho_{ij}=0$ and $z_{ij}\neq 0$,

$$\frac{d\bar{V}_{ij}}{da} = \frac{1}{2ac}\left[2\gamma + \psi_0\left(1 - \frac{z_{ij}}{2c}\right) + \psi_0\left(1 + \frac{z_{ij}}{2c}\right) - \frac{2c}{|z_{ij}|} + 2\ln(2qc) - 2\right]. \tag{A6}$$

For $\rho_{ij}\neq 0$,

$$\frac{d\bar{V}_{ij}}{da} = \frac{1}{ac}\left[\ln\left(\frac{q\rho_{ij}}{2}\right) + \gamma - 1\right] - \frac{2}{ac}\sum_{m=1}^{\infty}\cos\left(\frac{\pi m z_{ij}}{c}\right)K_0\left(\frac{\pi m \rho_{ij}}{c}\right). \tag{A7}$$

Here γ is the Euler-Mascheroni constant and $\psi_0(x)$ is a digamma function. The limit $q\to 0$ is assumed, and the divergent terms $\sim\ln(qa)$ are canceled by the charge-neutrality condition $\Sigma_i z_i = 0$.

[1] S. Iijima, Nature (London) **354**, 56 (1991).
[2] M. S. Dresselhaus, G. Dresselhaus, and P. C. Eklund, *Science of Fullerenes and Carbon Nanotubes* (Academic, New York, 1996).
[3] R. Saito, G. Dresselhaus, and M. S. Dresselhaus, *Physical Properties of Carbon Nanotubes* (Imperial College Press, London, 1998).
[4] D. Tomanek and R. J. Enbody, *Science and Application of Nanotubes* (Plenum, New York, 2000).
[5] D. Golberg, Y. Bando, C. C. Tang, and C. Y. Zhi, Adv. Mater. (Weinheim, Ger.) **19**, 2413 (2007).
[6] A. Rubio, J. L. Corkill, and M. L. Cohen, Phys. Rev. B **49**, 5081 (1994).
[7] X. Blase, A. Rubio, S. G. Louie, and M. L. Cohen, Europhys. Lett. **28**, 335 (1994).
[8] N. G. Chopra, J. Luyken, K. Cherry, V. H. Crespi, M. L. Cohen, S. G. Louie, and A. Zettl, Science **269**, 966 (1995).
[9] X. Blase, A. Rubio, S. G. Louie, and M. L. Cohen, Phys. Rev. B **51**, 6868 (1995).
[10] R. Z. Ma, Y. Bando, H. W. Zhu, T. Sato, C. L. Xu, and D. H. Wu, J. Am. Chem. Soc. **124**, 7672 (2002); S. H. Jhi, Phys. Rev. B **74**, 155424 (2006).
[11] D. Golberg, P. Dorozhkin, Y. Bando, M. Hasegawa, and Z.-C. Dong, Chem. Phys. Lett. **359**, 220 (2002); Y. B. Li, P. Dorozhkin, Y. Bando, and D. Golberg, Adv. Mater. (Weinheim, Ger.) **17**, 545 (2005).
[12] R. A. Jishi, L. Venkataraman, M. S. Dresselhaus, and G. Dresselhaus, Chem. Phys. Lett. **209**, 77 (1993).
[13] R. A. Jishi, M. S. Dresselhaus, and G. Dresselhaus, Phys. Rev. B **48**, 11385 (1993).
[14] R. A. Jishi, L. Venkataraman, M. S. Dresselhaus, and G. Dresselhaus, Phys. Rev. B **51**, 11176 (1995).
[15] E. Dobardžić, I. Milošević, B. Nikolić, T. Vuković, and M. Damnjanović, Phys. Rev. B **68**, 045408 (2003).
[16] D. Sánchez-Portal, E. Artacho, J. M. Soler, A. Rubio, and P. Ordejón, Phys. Rev. B **59**, 12678 (1999).
[17] P. C. Eklund, J. M. Holden, and R. A. Jishi, Carbon **33**, 959 (1995).
[18] D. Kahn and J. P. Lu, Phys. Rev. B **60**, 6535 (1999).
[19] O. Dubay and G. Kresse, Phys. Rev. B **67**, 035401 (2003); **69**, 089906(E) (2004).
[20] O. E. Alon, Phys. Rev. B **63**, 201403(R) (2001).
[21] M. Damnjanović, I. Milošević, T. Vuković, and R. Sredanović, Phys. Rev. B **60**, 2728 (1999).
[22] L.-H. Ye, B.-G. Liu, D.-S. Wang, and R. Han, Phys. Rev. B **69**, 235409 (2004).
[23] G. D. Mahan and G. S. Jeon, Phys. Rev. B **70**, 075405 (2004).
[24] G. S. Jeon and G. D. Mahan, Phys. Rev. B **72**, 155415 (2005).

[25] V. N. Popov, V. E. Van Doren, and M. Balkanski, Phys. Rev. B **61**, 3078 (2000).
[26] Y. N. Gartstein, Phys. Lett. A **327**, 83 (2004).
[27] J. Kürti, G. Kresse, and H. Kuzmany, Phys. Rev. B **58**, R8869 (1998).
[28] L. Henrard, E. Hernández, P. Bernier, and A. Rubio, Phys. Rev. B **60**, R8521 (1999).
[29] R. Saito, T. Takeya, T. Kimura, G. Dresselhaus, and M. S. Dresselhaus, Phys. Rev. B **57**, 4145 (1998).
[30] V. N. Popov, V. E. Van Doren, and M. Balkanski, Phys. Rev. B **59**, 8355 (1999).
[31] G. D. Mahan, Phys. Rev. B **65**, 235402 (2002).
[32] H. Suzuura and T. Ando, Phys. Rev. B **65**, 235412 (2002).
[33] J. Shiomi and S. Maruyama, Phys. Rev. B **73**, 205420 (2006); Phys. Rev. B **74**, 155401 (2006).
[34] D. Sánchez-Portal and E. Hernández, Phys. Rev. B **66**, 235415 (2002).
[35] V. N. Popov, Phys. Rev. B **67**, 085408 (2003).
[36] L. Wirtz, A. Rubio, R. A. de la Concha, and A. Loiseau, Phys. Rev. B **68**, 045425 (2003).
[37] C. Zhi, Y. Bando, C. Tang, D. Golberg, R. Xie, and T. Sekigushi, Appl. Phys. Lett. **86**, 213110 (2005).
[38] R. Arenal, A. C. Ferrari, S. Reich, L. Wirtz, J.-Y. Mevellec, S. Lefrant, A. Rubio, and A. Loiseau, Nano Lett. **6**, 1812 (2006).
[39] B. Akdim, R. Pachter, X. Duan, and W. W. Adams, Phys. Rev. B **67**, 245404 (2003).
[40] J.-F. Jia, H.-S. Wu, and H. Jiao, Physica B **381**, 90 (2006).
[41] H. J. Xiang, J. Yang, J. G. Hou, and Q. Zhu, Phys. Rev. B **68**, 035427 (2003).
[42] G. Benedek and G. Onida, Phys. Rev. B **47**, 16471 (1993).
[43] G. S. Jeon and G. D. Mahan, Phys. Rev. B **71**, 184306 (2005).